

Effect of Temperature on the Adsorption of Short Alkanes in the Zeolite SSZ-13—Adapting Adsorption Isotherms to Microporous Materials

Tao Jiang,[†] Florian Göttl,^{*,†} Rosa E. Bulo,[‡] and Philippe Sautet[†]

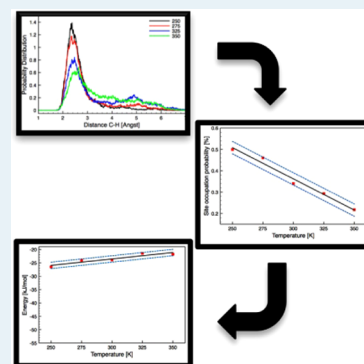
[†]Université de Lyon, CNRS, Ecole Normale Supérieure de Lyon, Laboratoire de Chimie, 46 Allée d'Italie, F-69342 Lyon Cedex 07, France

[‡]Inorganic Chemistry and Catalysis, Debye Institute for Nanomaterials Science, Utrecht University, Universiteitsweg 99, 3584 CG Utrecht, The Netherlands

S Supporting Information

ABSTRACT: Understanding the diffusion and adsorption of hydrocarbons in zeolites is a highly important topic in the field of catalysis in micro- and mesoporous materials. Especially, the properties of alkanes in zeolites have been studied extensively. A theoretical description of these processes is challenging, because two interactions are involved: the alkane physisorbs to the zeolite wall and chemisorbs weakly to the active centers. At room temperature, the alkane remains physisorbed almost all the time, but the chemical bond to the active sites is regularly broken. In this work, we study this behavior using *ab initio* molecular dynamics simulations for the adsorption of methane, ethane, and propane in SSZ-13, the zeolite with the smallest unit cell, at temperatures of 250, 275, 325, and 350 K. We find a temperature dependence of the adsorption energy and the probability of the alkane to be close to the active site, which corresponds to chemisorption. We derive a temperature-dependent expression for these probabilities or active site coverages, which have the energy difference between physisorbed and chemisorbed state as the main variable. The methodology derived in this work will be highly useful in correlating static electronic structure calculations to finite temperature coverages, which, following the Sabatier principle, is a key step to understand the performance of catalysts under reaction conditions and a prerequisite to computationally design such materials.

KEYWORDS: confinement effects, coverage, methane, ethane, propane, *ab initio* molecular dynamics



INTRODUCTION

Today, zeolites are among the most important industrial catalysts. Their micro- and mesoporous framework makes them highly selective,¹ which, combined with a high flexibility for the actual reactive centers, makes them promising candidates for a wide array of different chemical reactions.^{2–6} Currently, they play an important role in re-forming hydrocarbons in fluid catalytic cracking, a key process in the production of gasoline from crude oil. Zeolites are mainly composed of Si and oxygen, which form cornersharing tetrahedra and build a micro- and mesoporous framework. As soon as one of the Si atoms is substituted by Al, the framework is charged negatively. This is compensated by the presence of a positively charged counterion, which acts as a catalytically active center. This combination of channels, cavities, and active sites makes zeolites systems that, from a catalytic point of view, are similar to enzymes in nature.

Besides the necessity of determining the environment and therefore the chemical properties of these reactive centers, the key factors in understanding catalysis inside the zeolite framework are diffusion of molecules and accessibility of the active sites inside the materials.⁷ A first step in this direction is investigating the adsorption of simple hydrocarbons in zeolites.

Experimentally, it has been studied extensively, and it was found that free enthalpies of adsorption increase linearly with increased alkane chain length.⁹ Comparison between similar zeolite structures in their purely siliceous form and containing Al (and with it protons compensating the framework charge)¹⁰ shows a constant shift in free enthalpies of alkane adsorption.¹⁰ This led to the conclusion that the alkane adsorption is composed of two contributions, namely, a weak chemical bond between the alkane and the active site and van der Waals (vdW) interactions between alkane and zeolite walls. Although chemisorption strength is constant, the vdW interactions increase with every CH₂ group, with the slope depending on the shape of the cavity, and can be related to the density of the material.⁸

Because all processes take place inside the material, it is highly challenging to obtain a detailed atomistic picture using only experimental measurements. Therefore, different theoretical methods have been used to describe both diffusion and adsorption.⁷ One way is to use models based upon classic

Received: February 12, 2014

Revised: June 10, 2014

Published: June 11, 2014

potentials. This allows us to draw conclusions about shape-selectivity,¹ physisorption minima,¹² or diffusion properties inside the material.⁷ The simple nature of the model allows an efficient and fast treatment of very large systems, but chemical reactions cannot be described explicitly.

Another approach is to use electronic structure calculations. However, the most common approaches based upon semilocal correlation expressions within density functional theory can not capture nonlocal vdW interactions.⁹ Nonlocal interactions are included in many high-level methods in quantum chemistry and solid state physics. Such methods are typically demanding and restricted to small-cell zeolites^{11,15,16} or small to medium sized clusters cut out of the material for modeling more complex structures.^{13,14} VdW interactions are long ranged and require the treatment of fully periodic systems. Therefore, substantial work has been invested in finding nonlocal density functional theory based methods, which are able to describe such long-ranged forces appropriately,^{19–22} and they have been tested for alkane adsorption in zeolites.^{11,15–18}

However, comparing calculated results to experiment is not straightforward.¹¹ Typically, free enthalpies of adsorption are measured at finite temperature. Because the bond between alkanes and the active site is comparatively weak, it can be broken easily, and the alkane will diffuse through the cavity. To describe this process appropriately, Bučko et al. performed ab initio molecular dynamics calculations for propane in SSZ-13 at different temperatures.²³ They then defined adsorption (a state in which the catalytic reaction can occur) as the ensemble of configurations, where one carbon atom in the molecule was closer than 3 Å to the active site. On the basis of this work, we followed a similar methodology for different alkanes in zeolites at 300 K, refined the adsorption cutoff to 2.5 Å, and developed a scheme to extrapolate 0 K calculations to finite temperature.¹¹ Another approach was taken by Swisher et al.²⁴ and Tranca et al.²⁵ who used Monte Carlo calculations based upon classical force fields to determine the same quantity.

Although the extrapolation of static calculations to finite temperature is already very important, finding an expression of the occupation probability of active sites might be even more crucial from a catalytic point of view. Following the Sabatier principle, molecules can only react when they adsorb sufficiently strongly to be close to the active site often enough and weakly enough so that possible products can still desorb. Therefore, it is a key feature to dynamically understand the concept of active site occupation to predict the activity of a catalyst under certain experimental conditions.

For this reason, we investigate the adsorption of methane, ethane, and propane at 250, 275, 325, and 350 K using ab initio molecular dynamics calculations. We evaluate average adsorption energies, active site occupation, and structural properties. We use this information to develop a model and a general expression for adsorption isotherms in microporous systems based upon static calculations and geometric considerations. Following the Sabatier principle and volcano relationships, such an expression is the basis to relate chemical activity of a catalyst to reaction conditions.

RESULTS

As already discussed above, the interactions of alkanes with zeolites depend on two different contributions. The alkane is bound to the cavity wall by weak vdW interactions while it also forms a weak chemical bond with the Brønsted acid sites. At room temperature, the alkane can break this chemical bond

regularly and move through the cavity, leaving it chemisorbed to the active site for a certain amount of time while thermal motion allows it to move through the cavity in the remaining time. It can be expected that temperature influences this behavior. Therefore, we performed calculations for the adsorption of the alkanes at temperatures of 250, 275, 325, and 350 K and included the values published in literature for 300 K.⁶ Typically this diffusion is modeled using classic force fields. In this work, however, we are not only interested in the description of diffusion but also in the interactions between the alkane and the Brønsted acid site, which is highly sensitive to the exact parametrization of the force fields. To be able to relate the dynamic results to static density functional theory calculations, we chose to use ab initio molecular dynamics simulations to model the thermal motion of the molecule.

For methane (see Figure 1a), the inner energy of adsorption decreases by almost 5 kJ/mol, or almost 20% over the temperature range. This corresponds to changes in the probability distribution of the distances between the C atom and the Brønsted acid site, which is displayed in Figure 1b. Its maximum corresponds to the bonded molecule for distances between 2 and 2.5 Å, and this maximum probability decreases with increased temperature, while it is at the same time shifted to slightly larger distances. The decrease in probability at the maximum is compensated by a higher probability for the molecule to be found at larger distances. As discussed in previous work, we will consider the molecule to be adsorbed as long as this distance is smaller than r (see Figure S2 in the Supporting Information (SI)). In the literature, r values of 2.5 and 3.0 Å have been suggested. A more detailed discussion of the impact of this choice is given in the SI, and in the following, values for $r = 2.5$ Å, followed by values for $r = 3$ Å in brackets, will be given. Figures for $r = 3$ Å are shown in Figure S4 in the SI. It is important to note that although absolute values change with respect to this parameter, the general trends remain unchanged. This probability to be chemisorbed decreases from almost 50% (83%) to 22% (46%) over the studied temperature range (see Figure 1c). We also calculated confidence intervals (95%) for those two values, and both show a very good linear dependence with errors of less than 1.5 kJ/mol and 3% (3%).

For ethane, we find similar trends. The overall decrease of inner energies of adsorption over the temperature range, however, is less than 2 kJ/mol. A linear fit increases the differences to 3 kJ/mol (see Figure 2a). The distance between the C atom of methane and the proton at the Brønsted site (see Figure 2b, defined as the minimum distance between one of the C atoms and the proton) shows very similar general trends compared to methane. It is however important to point out that we find a higher probability for the alkane to stay close to the active site for 275 K compared to 250 K. Since molecular dynamics simulations are statistical methods, such behavior must be expected due to finite sampling times. Also the long carbon–proton distance tail of the distribution does not reach as far, which can be attributed to the different sizes of the molecule. Again the probability of finding ethane close to the active site decreases significantly from 43% (69%) to 27% (54%) over the temperature range (see Figure 2c). It is necessary to mention that the confidence intervals are far larger for the case of ethane and that they are close to 2 kJ/mol for the inner energy of adsorption and almost 10% (15%) for the chemisorption probability.

The picture for propane is again very similar. The inner energy of adsorption decreases as a function of temperature

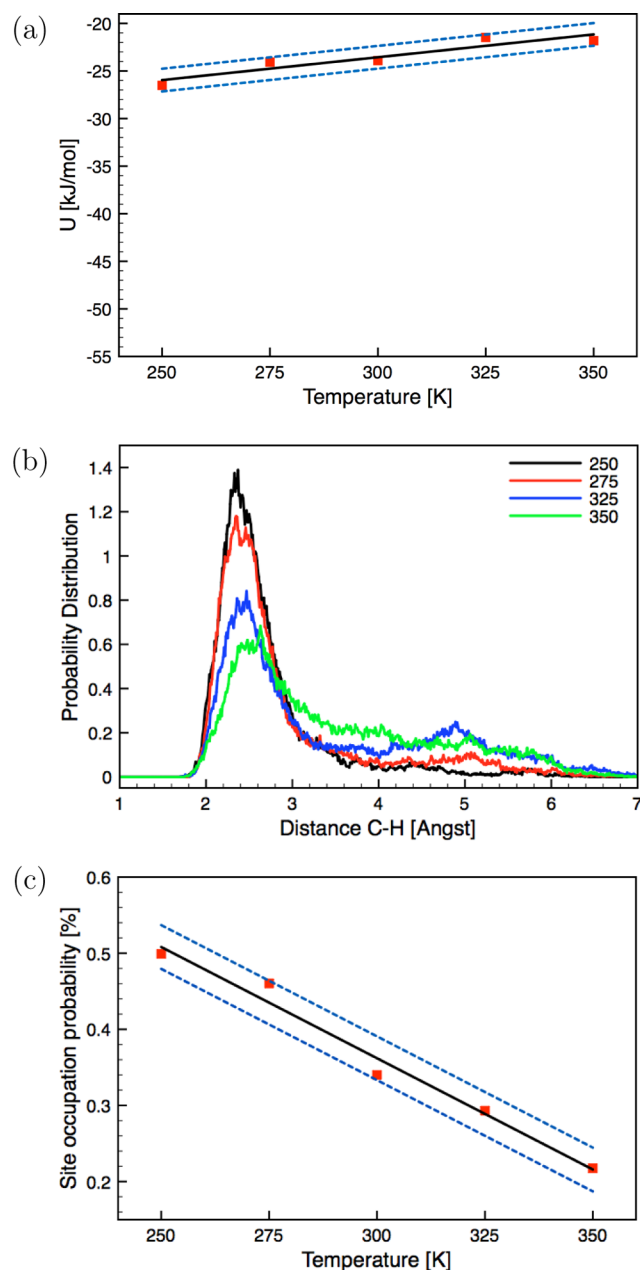


Figure 1. Adsorption energy (a), the methane carbon–zeolite proton distance distribution (b), and the probability to be close to the active site (c) for methane. In (a) and (c), the red rectangles denote the data points, the black line the linear regression, and the dashed blue lines the confidence intervals for the data. In (b), different colors correspond to the probability distribution at different temperatures (black at 250 K, red at 275 K, blue at 325 K, and green at 350 K).

from 52 kJ/mol (250 K) to 46 kJ/mol (350 K), and this is rather similar for both the fitted values and the interpolation (see Figure 3a). The maximum in the distance distribution is similar to methane (see Figure 3b), and we find a small side-maximum at 350 K at about 3.7 Å. The tail of the distribution in the region of long carbon–proton distances is even more reduced compared to ethane. This can be expected, because propane is larger, and therefore, the minimum distances between one of its C atoms and the active site must be smaller. A similar picture emerges for the probability of finding a chemisorbed state (see Figure 3c). It decreases from 49% (83%) (250 K) to 23% (52%) (350 K) as a function of

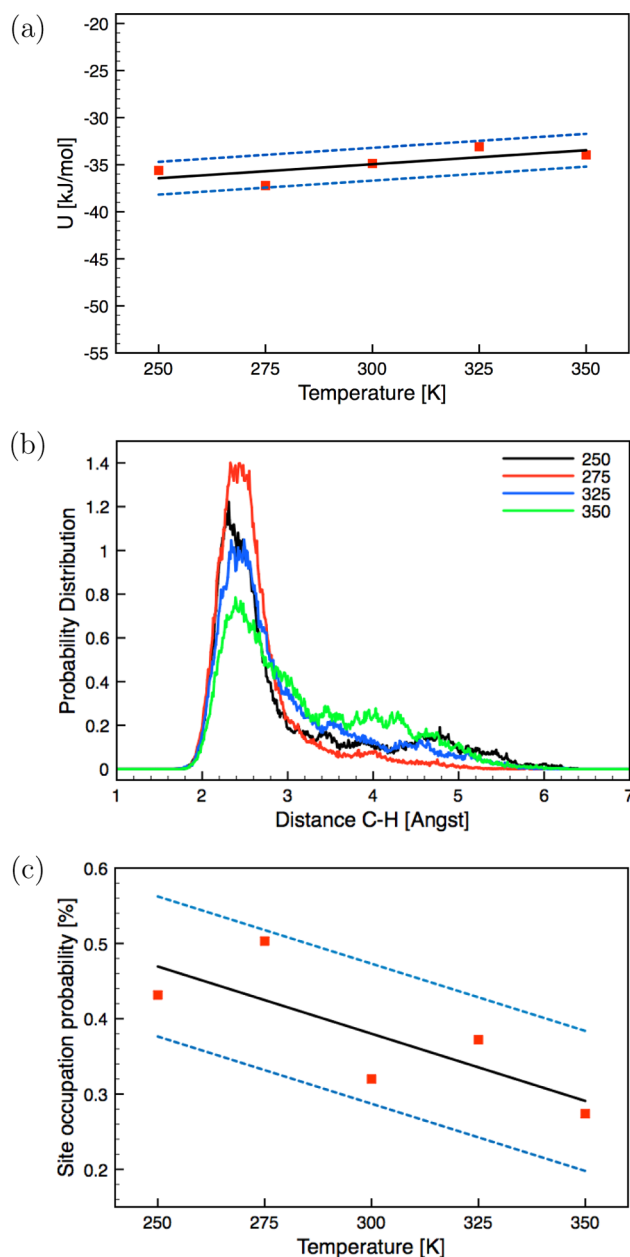


Figure 2. Adsorption energy (a), the carbon–proton distance distribution (b), and the probability to be close to the active site (c) for ethane. The color code is explained in Figure 1.

temperature for the actual data and from 52% (86%) to 37% (68%) for the extrapolation. Compared to the case of ethane, the confidence is slightly increased for the inner energy of adsorption (almost 2.5 kJ/mol) and decreased for the adsorption probability (less than 5% (9%)).

Additionally, it is important to isolate the bonding energy between the active site and the alkane. For that reason, we calculated the inner energies of the system as a function of the distance between the closest carbon atom in the alkane and the acid site proton and formed averages for every 0.1 Å increment. We then defined the chemisorption energies as the difference between the lowest and the highest value along the profile. The obtained values were averaged over the temperature from 250 to 350 K yielding chemisorption energy values of −11 kJ/mol for methane, −15 kJ/mol for ethane, and −16 kJ/mol for propane. The spread of those values upon temperature is

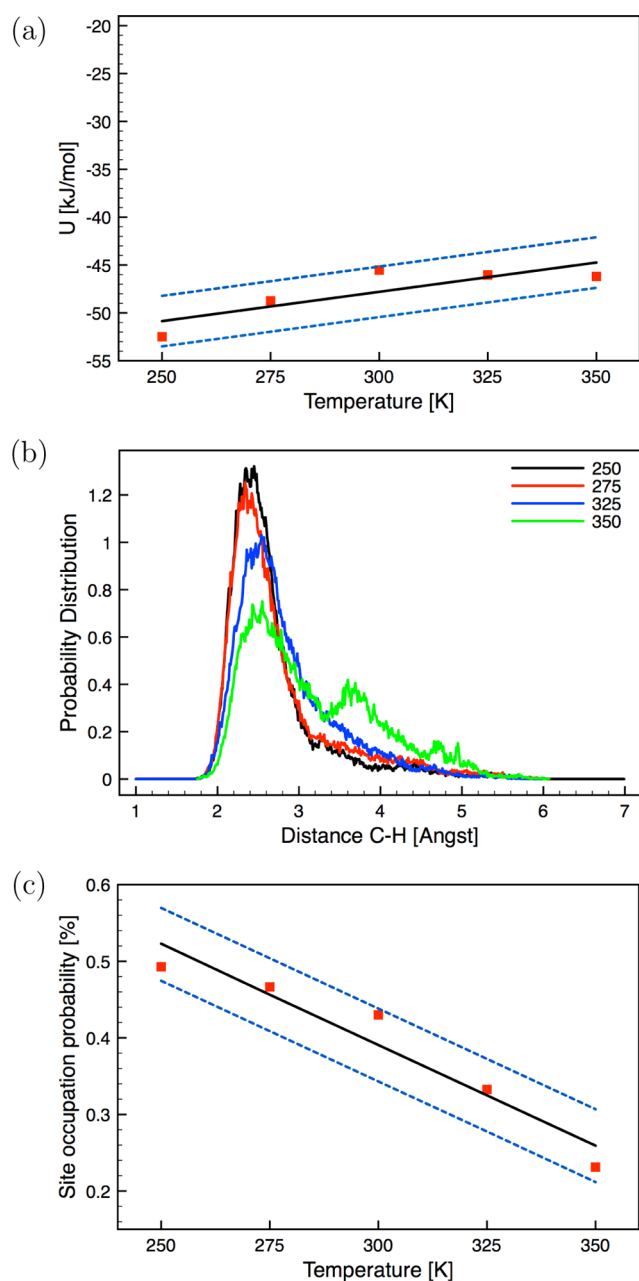


Figure 3. Adsorption energy (a), the carbon–proton distance distribution (b), and the probability to be close to the active site (c) for propane. The color code is explained in Figure 1.

comparatively small for methane (−10 to −12 kJ/mol) and ethane (−13 to −16 kJ/mol), whereas it is larger for propane (−8 to −22 kJ/mol). These values are only slightly smaller than statically calculated numbers of −14 kJ/mol for methane, −16 kJ/mol for ethane, and −17 kJ/mol for propane.¹¹ Considering the averaging over thousands of configurations and the neglect of zero point vibrations in the statical calculations, this can be seen as an almost perfect agreement.

Because the calculations were performed in the canonical ensemble, it is also possible to calculate the radially dependent free energies of adsorption as $F(r) = -kT \ln P(r)$, where $P(r)$ is the probability distribution function displayed in panel b of Figures 1, 2, and 3. In all free-energy curves, we find a clear adsorption minimum. However, they are even more sensitive to exact convergence than the initial $P(r)$ curves, which leads to a

large noise for r values larger than 4 Å. For that reason, we calculate the free energy of adsorption between the minimum and $F(r = 4)$. This leads to free energies of chemisorption (F_{chem}) values of 7, 6, 5, 6, and 4 kJ/mol for methane (for temperatures of 250, 275, 300, 325, and 350 K), 5, 7, 4, 6, and 3 kJ/mol for ethane, and 7, 6, 7, 6, and 3 kJ/mol for propane. These values are considerably lower than the inner energies of chemisorption, which can be traced back to an expected decrease of entropy upon adsorption. We find the expected decrease in F for increased temperature,³⁹ which now allows us to calculate the entropy as slope of a linear fit. We find ΔS_{chem} values of $-27 \pm 10 \text{ J mol}^{-1} \text{ K}^{-1}$ for methane, $-17 \pm 17 \text{ J mol}^{-1} \text{ K}^{-1}$ for propane, and $-30 \pm 14 \text{ J mol}^{-1} \text{ K}^{-1}$ for propane. These values are significantly smaller than the values between 55 and 60 $\text{J mol}^{-1} \text{ K}^{-1}$ found by Tranca et al. for propane in the given temperature range.²⁵ This is expected, because we focus on the entropy of chemisorption, whereas the other entropy values are found for the global process, which includes significant contributions from alkane diffusion through the cavity.

Similar to the adsorption probability of the alkane to the active site proton, it is also possible to define the distance to the closest framework Si atoms of the zeolite. These distributions (given in Figure S1 in the SI) show a maximum at about 4 Å. This indicates that in the given temperature range, the alkane almost always remains close to the cavity wall and can only rarely break the vdW forces and desorb to move toward the center of the cavity. The slight shift of the curve for methane to larger values indicates that these events are more likely to happen at higher temperatures for the more weakly bonded methane.

Additionally, we want to point out that for all temperatures, we find an increase of inner energies of adsorption with alkane length. This effect can mainly be traced back to an increase in the vdW interactions with the zeolite wall for increased alkane chain length, because we already showed above that the actual interaction strength with the active site hardly varies.

These results illustrate that we find the right trends but that errors for the probabilities to find the alkane close to the active site and with it the variance in the inner energies of adsorption and free energies of chemisorption are fairly large. It is well-known that the convergence of free-energy calculations, especially when significant barriers have to be overcome, requires more sophisticated methods and extensive sampling times.³⁷ However, in the studied temperature range, the bond between the alkane and the active site is broken regularly, an indication that standard MD is adequate to describe this problem. However, molecular dynamics simulations of 150 ps might not suffice to arrive at the ergodic limit. To address these issues (a more detailed discussion can be found in the SI) and to have an estimate for the errors due to limited simulation time, we performed 10 runs for 1 ns each to determine the motion of propane in SSZ-13 at 350 K using classical force fields and compared values for free energies and coverage (for a cutoff of 2.5 and 3 Å) at the end of the run and after 150 ps. We found that errors for both values roughly double for the shorter run time. We find standard deviations of about 3% for the free energy for the 150 ps runs. The coverage seems to be a more sensitive parameter, and we find a standard deviation of about 10% for the shorter runs. These error bars show very good agreement with our confidence intervals, which indicates that they are a good measure to assess the quality of our results.

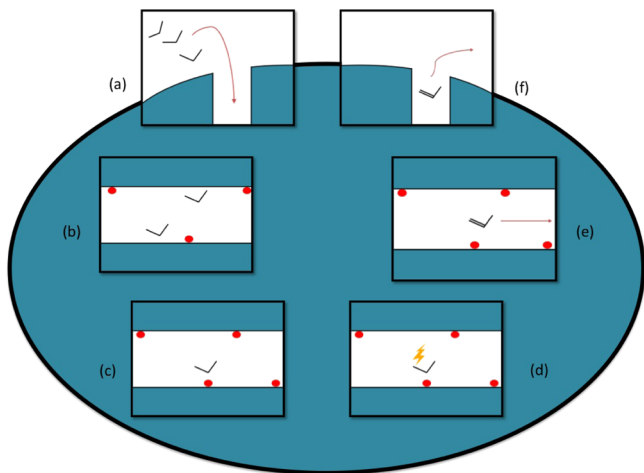
DISCUSSION

In this work, we find a clear dependence on the temperature of the average adsorption energies at the active site, and the actual change over the investigated temperature range is in excellent agreement with data reported in literature.^{26,25} Our results clearly show that at finite temperature, the bond between the alkane and the active site can regularly be broken, which leads to a diffusion of the alkane along the wall of the cavity. Although the results on alkane movement inside the zeolite obtained in this work are already interesting per se, one further goal is to relate them to the standard models in catalysis, which would allow us to circumvent highly expensive ab initio MD simulations and address these effects using static calculations.

As already discussed by Bučko et al., a chemical reaction is only possible if the reactant is reasonably close to the catalytically active sites in the zeolite.²³ Defining a cutoff radius allows the calculation of a probability for the alkane to be close to the active site from molecular dynamics simulations, which can then either be used as an input to determine reaction rates or to calculate finite temperature inner energies of adsorption in the microporous material.

Let us now describe the pathway of the molecule in the porous network (see Scheme 1). As soon as the alkane enters

Scheme 1. Pathway of the Molecule in the Porous Network^a



^aAfter the alkane enters the porous structure (a), it will diffuse along the inner wall of the zeolite cavities (b) until it reaches the catalytically active site (c). At these sites, reactions take place, and the product is formed (d). After this reaction, the products desorb from the active sites (e) and leave the zeolite.

the zeolite pore, it is in a preadsorbed state to the zeolite cavity. The probability to be close to a catalytically active site, however, is equivalent to the coverage θ used in the standard models of catalysis. In equilibrium, the probability to adsorb and desorb will be equal.

Under the assumption of a barrierless process, the adsorption rate at a catalytically active site will mainly depend on the amount of the inner surface covered by the alkane (A/S , where A denotes the area covered by the alkane and S the inner surface area of the zeolite) and the amount of available catalytically active sites per surface area (n/S , with n being the amount of active sites, see Figure S2 in the SI)

$$r_A = a \frac{A}{S} \frac{n}{S} (1 - \theta) \quad (1)$$

with the prefactor a describing the accessibility of the active site for the alkanes.

At the same time, the actual desorption will depend on the coverage of the sites and the desorption probability

$$r_d = b e^{-G_{\text{chem}}/kT} \theta \quad (2)$$

where G_{chem} denotes the Gibbs free energy of chemisorption of the alkane to the active site, which has to be overcome in the desorption, and b is an Arrhenius prefactor.

In equilibrium adsorption and desorption rates are equal, which leads to

$$\theta = \frac{B \frac{A}{S} \frac{n}{S} e^{+G_{\text{chem}}/kT}}{1 + B \frac{A}{S} \frac{n}{S} e^{+G_{\text{chem}}/kT}} \quad (3)$$

where B is a/b .

Clearly the amount of surface area covered by the alkane will be related to the pressure outside the zeolite, and therefore, the reaction conditions.³⁸ However, to establish the dependence on this factor is not easy, because the outer surface and the diffusion into the pores will lead to large changes in the final amount of gas adsorbed in the zeolite. The density of active sites on the surface is again a material parameter and is connected to the total number of active sites.

Taking this into account, the equations derived in this work closely resemble the standard adsorption isotherms discussed in many physical chemistry of catalysis textbooks. However, there is a subtle but decisive difference. Typically, the enthalpy of adsorption of the molecule with respect to the gas phase reference is used; however, in microporous materials, it is the Gibbs free energy of chemisorption (see Figure 4).

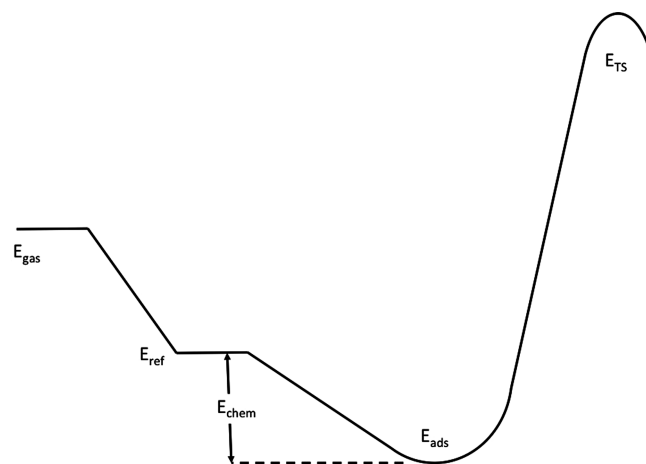


Figure 4. After entering the pore, the alkane will be in a preadsorbed state with energy E_{ref} . As discussed in the text and displayed in eq 1, the alkane will further adsorb to the active site (with energy E_{ads}) before a reaction can take place. In this work, we show that it is actually the difference between these two energies, the chemisorption energy E_{chem} , which should be considered to determine coverages and adsorption isotherms in zeolites.

Rewriting 3 leads to

$$\frac{\theta_T}{1 - \theta_T} = B \frac{A}{S} \frac{n}{S} e^{+G_{\text{chem}}/kT} \quad (4)$$

which can easily be rewritten to

$$B = \frac{S}{A} \frac{S}{n} \frac{\theta_T}{1 - \theta_T} e^{-G_{\text{chem}}/kT} \quad (5)$$

From this equation, it is now possible to determine the prefactor B , by substituting G_{chem} by F_{chem} , the free energy of chemisorption, the corresponding quantity in molecular dynamics simulations at constant volume. Additionally, it is important to take into account the change in projected surface area of the alkane (when considering spheres surrounding the alkanes this leads to an increase in the covered surface area between methane and propane from 39.27 \AA^2 to 81.21 \AA^2 for a radius of 2.5 \AA and from 56.55 \AA^2 to 116.94 \AA^2 for a radius of 3 \AA). In addition, the accessible surface area will also vary with molecular geometry. Defining a general expression for the geometry of different molecules is very challenging, but, when considering the accessibility of different areas of the zeolite, for the comparatively large pores of SSZ-13, differences between methane and propane can be assumed to be small. For the sake of simplicity of the argument, we will assume that the accessibility stays constant and will use data from the literature for molecules with 4 \AA diameter (an accessible surface area of $273 \text{ \AA}^2/\text{unit cell}$).²⁷

Using these parameters and the free energy of chemisorption values determined above leads to B values of 108 ± 15 , 105 ± 45 , and 51 ± 12 for methane, ethane, and propane, respectively, and to values of 249 ± 40 , 247 ± 150 , and 109 ± 70 for coverage values obtained with cutoff parameters of 2.5 and 3 \AA , respectively. The error bars in these calculations are relatively large and they seem to be very sensitive to ergodicity. They show a dependence on the choice of the cutoff parameter, but similar trends emerge. For methane and ethane, we find almost equivalent B values. For propane, it is significantly reduced. This can be traced back to differences in the accessibility of the different CH_x groups between those molecules. Although the terminal groups in the molecules are very similar, accessing the central CH_2 group in propane is far more difficult, which leads to this decrease. Bučko et al. already noticed this effect, which allowed them to explain the product selectivity in the case of alkane dehydrogenation.²³

Considering the high computational demands for ab initio molecular dynamics simulations and that also larger zeolite unit cells than the one treated in this work are of high interest, it is desirable to substitute G_{chem} by U_{chem} , which can be accessed from static calculations. Hence we rewrite

$$G_{\text{chem}} = U_{\text{chem}} - TS_{\text{chem}} \quad (6)$$

with S_{chem} being the change in entropy upon adsorption. This leads to a coverage expression which depends on the prefactor B , the loss of entropy upon chemisorption, and the chemisorption strength. Though our calculations are not fully enough converged to make strong statements about B and S , Swisher et al. developed a model similar to this work, where they used Monte Carlo (MC) simulations with a classical force field to calculate occupation probabilities of different types of active sites in MFI and FAU structures.²⁴ Additionally, Tranca et al. have shown that it is also possible to use a similar methodology to quantify entropy contributions for such systems.²⁵ Whereas they studied the total catalytic reaction, which includes the description of alkane cracking, the model presented in this work focuses on the coverage of the active sites and explicitly highlights the importance of the chemisorption energy in this context. Combining these approaches will allow us to access B and S values from classical

force-field calculations and refine those calculations by static electronic structure calculations for the adsorption strength. Such a refinement becomes important in describing the adsorption to different types of active sites in similar framework positions, such as TM atoms exchanged in zeolite structures.

The coverages calculated in this work can also be used to calculate finite temperature inner energies of adsorption using

$$U(T) = U_{\text{phys}} + \theta_T U_{\text{chem}} \quad (7)$$

Comparing the results from molecular dynamics calculations and extrapolations for coverage values for cutoffs of 2.5 and 3 \AA (as displayed in the SI) shows that, while the general trends are preserved in both cases, extrapolations using the smaller cutoff lead to better agreement with MD simulations. To demonstrate the power of this combined approach, we used the derived parameters and eqs 3 and 7 to calculate the inner energy of adsorption for propane between temperatures 100 and 700 K (see Figure 5). At 100 K , where the alkane is always adsorbed

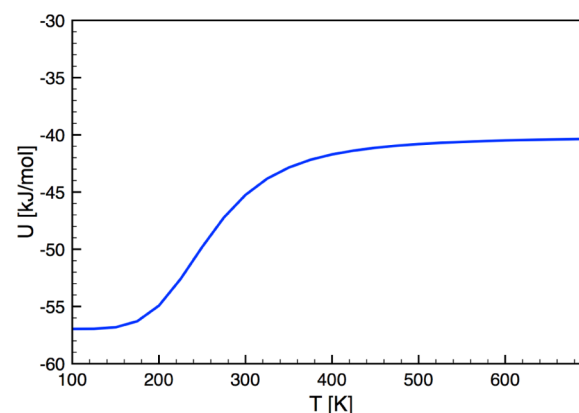


Figure 5. Methodology developed in this work allows the extrapolation of inner energies of adsorption of alkanes over a wide temperature range. In this figure, we demonstrate this temperature range for the adsorption of propane. We find a variation of about 17 kJ/mol over the whole temperature range, which is very different from the assumption of a constant value made in many studies.

to the active site, we find an adsorption energy of -57 kJ/mol . When the temperature starts to rise, the free energy of adsorption is lowered, which corresponds to a higher probability for the alkane to be away from the active site in the trajectory. Above 400 K , the U starts to reach about -40 kJ/mol , which corresponds to the regime where the alkane–active site bond can be broken and re-formed at a high rate. Comparing the data to the classical Monte Carlo simulations of Tranca et al.²⁵ of propane in ZSM-5, we find very similar qualitative behavior. This demonstrates that it is valid to use the discussed extrapolation approach. Another important point to note is that especially close to room temperature, the inner energy of adsorption (and with it the enthalpy of adsorption) varies significantly. This is especially important in experimental measurements, where data is extrapolated under the assumption of a constant enthalpy of adsorption, which, as we demonstrate here, is not a valid hypothesis. In the future, the model developed in this work will lead to more sophisticated extrapolation schemes and should allow a more exact determination of the different factors in the alkane adsorption process.

CONCLUSIONS

In this work, we present molecular dynamics calculations for the adsorption of the short alkanes methane, ethane, and propane in the protonated zeolite SSZ-13. From the obtained data, we investigate finite temperature adsorption energies and active site occupation probabilities. For temperatures between 250 and 350 K, we find that the alkane diffuses along the inner surface of the zeolite and enters a chemisorbed state. At all temperatures, this bond can be broken on a picosecond time scale. In this paper, we developed a model to arrive at the site occupation probability (or coverage), which depends only on the chemisorption strength to the active site and not on the more or less constant van der Waals interactions with the zeolite wall.

The results presented in this work allow the calculation of finite temperature site occupations (coverages) for different zeolite structures on the basis of static calculations and structural considerations. Following the Sabatier principle and volcano relationships, the methodology developed here is a key step in understanding the catalytic activity of microporous materials in different reaction conditions, the underlying fundamentals of industrial catalyst design.

METHODS

In this work, we perform ab initio molecular dynamics simulations using the Vienna Ab-Initio Simulation Package.^{29,30} This is a plane-wave code using PAW pseudopotentials³¹ in the framework of Kresse and Joubert.³² To calculate the internuclear forces, we used the semilocal PBE density functional³³ combined with the DFT-d(2) method of Grimme,³⁴ to take the vdW interaction into account. We applied an energy cutoff of 400 eV for the plane-wave basis and restricted the sampling of the unit cell to the Γ -point. In our MD simulations, we used a time step of 1 fs and the Andersen thermostat³⁵ to take finite temperature effects in a canonic ensemble into account. We set the probability to change the velocity of the particles to roughly $1/n$, where n represents the atom number in the unit cell. The total sampling time was 150 ps, a time scale within reach of ab initio molecular dynamics simulations, where the alkane typically stays within one cavity so that problems with intercavity diffusion are avoided.

In our simulations, we used a double unit cell of SSZ-13, which consists of 24 symmetrically equivalent T-sites. Most of them are occupied by Si, but one is substituted by Al. Contrary to other zeolite structures, all Si positions are symmetrically equivalent; therefore, the system is not sensitive to the choice of Al position. The exact data of the unit cell is given in ref 11. We then inserted methane, ethane, and propane in the unit cell. We calculate the adsorption inner energies of the alkanes as

$$U_{\text{ads}}^T = \langle U \rangle_{(\text{Chab}+\text{alk})}^T - \langle U \rangle_{(\text{Chab})}^T - \langle U \rangle_{(\text{alk})}^T \quad (8)$$

where the brackets include the average energy at temperature T for the different subsystems, which include the chabazite, chabazite + alkane, and the alkane alone.

To check convergence of the ab initio molecular dynamics simulations, we performed classic force-field calculations using the LAMMPS code and a force field based upon the literature³⁶ for an 8 times larger cell. To arrive at stable molecular dynamics results, we adapted the Morse potential to a harmonic potential, while keeping the same minima, but with force constants from the CHARMM force field ($k_{\text{OH}} = 505.0 \text{ kcal/mol/\AA}^2$, $k_{\text{CH}} =$

$322.0 \text{ kcal/mol/\AA}^2$, $k_{\text{CC}} = 222.5 \text{ kcal/mol/\AA}^2$) and a charge of +0.15 on the hydrogen atoms.

ASSOCIATED CONTENT

Supporting Information

More detailed discussions of the framework—alkane distances, the choice of the cutoff parameters when calculating the coverage, and estimation of errors due to finite sampling times are given in the Supporting Information. This material is available free of charge via the Internet at <http://pubs.acs.org/>.

AUTHOR INFORMATION

Corresponding Author

*E-mail: florian.goltl@ens-lyon.fr

Notes

The authors declare no competing financial interest.

ACKNOWLEDGMENTS

F.G. and P.S. acknowledge support within the ANR project DYQUA.

REFERENCES

- (1) Smit, B.; Maesen, T. L. M. *Nature* **2008**, *451*, 671–678.
- (2) Woertink, J. S.; Smeets, P. J.; Groothaert, M. H.; Vance, M. A.; Sels, B. F.; Schoonheydt, R. A.; Solomon, E. I. *Proc. Nat. Acad. Sci. U.S.A.* **2009**, *106*, 18908–18913.
- (3) Sastre, F.; Corma, A.; Garcia, H. J. *Am. Chem. Soc.* **2012**, *134*, 14137–14141.
- (4) Hemelsoet, K.; Qian, Q.; De Meyer, T.; De Wispelaere, K.; De Sterck, B.; Weckhuysen, B. M.; Waroquier, M.; Van Speybroeck, V. *Chem.—Eur. J.* **2013**, *19*, 16595–16606.
- (5) Hammond, C.; Conrad, S.; Hermans, I. *ChemSusChem* **2012**, *5*, 1668–1686.
- (6) Göttl, F.; Buló, R. E.; Hafner, J.; Sautet, P. *J. Phys. Chem. Lett.* **2013**, *4*, 2244–2249.
- (7) Smit, B.; Maesen, T. L. M. *Chem. Rev.* **2008**, *108*, 4125–4184.
- (8) Eder, F.; Lercher, J. A. *J. Phys. Chem. B* **1997**, *101*, 1273–1278.
- (9) Benco, L.; Demuth, T.; Hafner, J.; Hutschka, F.; Toulhoat, H. *J. Chem. Phys.* **2001**, *114*, 6327–6334.
- (10) Eder, F.; Lercher, J. A. *J. Chem. Phys.* **1996**, *100*, 16460–16462.
- (11) Göttl, F.; Hafner, J. *Microporous Mesoporous Mater.* **2013**, *166*, 176–184.
- (12) Kim, J.; Maiti, A.; Lin, L. C.; Stolaroff, J. K.; Smit, B.; Aines, R. D. *Nat. Commun.* **2013**, *4*, 1694.
- (13) Tuma, C.; Sauer, J. *Chem. Phys. Lett.* **2004**, *387*, 388–394.
- (14) Tuma, C.; Sauer, J. *Phys. Chem. Chem. Phys.* **2006**, *8*, 3955–3965.
- (15) Göttl, F.; Hafner, J. *J. Chem. Phys.* **2011**, *134*, 064102.
- (16) Göttl, F.; Grüneis, A.; Bučko, T.; Hafner, J. *J. Chem. Phys.* **2012**, *137*, 114111.
- (17) Brogaard, R. Y.; Moses, P. G.; Nørskov, J. K. *Catal. Lett.* **2012**, *142*, 1057–1060.
- (18) Göttl, F.; Sautet, P. *J. Chem. Phys.* **2014**, *140*, 154105.
- (19) Dion, M.; Rydberg, H.; Schröder, E.; Langreth, D. C.; Lundqvist, B. I. *Phys. Rev. Lett.* **2004**, *92*, 246401.
- (20) Gulans, A.; Puska, M. J.; Nieminen, R. M. *Phys. Rev. B* **2009**, *79*, 201105.
- (21) Klimeš, J.; Bowler, D.; Michaelides, A. *Phys. Rev. B* **2011**, *83*, 195131.
- (22) Wellendorff, J.; Lundgaard, L. T.; Mogelhøj, A.; Petzold, V.; Landis, D. D.; Nørskov, J. T.; Bligaard, T.; Jacobsen, K. W. *Phys. Rev. B* **2012**, *85*, 235149.
- (23) Bucko, T.; Benco, L.; Hafner, J.; Angyan, J. T. *J. Catal.* **2011**, *279*, 220–228.
- (24) Swisher, J. A.; Hansen, N.; Maesen, T.; Keil, F. J.; Smit, B.; Bell, A. T. *J. Phys. Chem. C* **2010**, *114*, 10229–10239.

- (25) Tranca, D. C.; Hansen, N.; Swisher, J. A.; Smit, B.; Keil, F. J. *J. Phys. Chem. C* **2012**, *116*, 23408–23417.
- (26) De Moor, B. A.; Reyniers, M.-F.; Gobin, O. C.; Lercher, J. A.; Marin, G. B. *J. Phys. Chem. C* **2011**, *115*, 1204.
- (27) First, E. L.; Gounaris, C. E.; Wei, J.; Floudas, C. A. *Phys. Chem. Chem. Phys.* **2011**, *13*, 17339–17358.
- (28) Bučko, T.; Benco, L.; Dubay, O.; Dellago, C.; Hafner, J. *J. Chem. Phys.* **2009**, *131*, 214508.
- (29) Kresse, G.; Hafner, J. *Phys. Rev. B* **1993**, *48*, 13115–13118.
- (30) Kresse, G.; Furthmüller, J. *Comput. Mater. Sci.* **1996**, *6*, 15–50.
- (31) Blöchl, P. E. *Phys. Rev. B* **1994**, *50*, 17953–17979.
- (32) Kresse, G.; Joubert, D. *Phys. Rev. B* **1999**, *59*, 1758–1775.
- (33) Perdew, J. P.; Burke, K.; Ernzerhof, M. *Phys. Rev. Lett.* **1996**, *77*, 3865–3868.
- (34) Grimme, S. *J. Comput. Chem.* **2006**, *27*, 1787–1799.
- (35) Andersen, H. J. *J. Chem. Phys.* **1980**, *72*, 2384–2393.
- (36) Titiloye, J. O.; Parker, S. C.; Stone, F. S.; Catlow, C. R. A. *J. Phys. Chem.* **1991**, *95*, 4038–4044.
- (37) Chipot, C. *WIREs Comput. Mol. Sci.* **2014**, *4*, 71–89.
- (38) At higher temperatures, when the alkane regularly desorbs from the inner zeolite surface, this will correspond to the amount of volume occupied by the alkane, which again is directly related to the pressure.
- (39) In general, the free energy corresponds to $F = U - TS$. For constant entropy S , it will decrease with increased temperature T . Additionally, the S will increase with increased T , which leads to an even larger decrease in F .